An Efficient Numerical Spectral Domain Method to Analyze a Large Class of Nonreciprocal Planar Transmission Lines

Francisco Mesa, Ricardo Marques, and Manuel Horno *Member, IEEE*

Abstract—**This paper presents an efficient numerical application of the Galerkin method in the spectral domain, (SD), to the analysis of strip-like/slot-like coplanar transmission lines embedded in a bianisotropic multilayered medium. The method is based on the obtaining of the spectral dyadic Green's function by the equivalent boundary method (EBM), a suitable third order extraction technique of the asymptotic behavior of the Green's dyad, an enhanced numerical integration scheme and the use of an adequate contour integral method for searching zeros in the complex plane. This method, namely the SD-EBM, has been found to be very suitable to analyse transmission lines with semiconductor and/or ferrites magnetised at an arbitrary direction, including the study of magnetostatic wave propagation phenomena.**

I. Introduction

THE GREAT role played by the nonreciprocal devices in the microwave technology from early was supported by an extense theoretical investigation on inhomogeneously ferrite loaded waveguide [1]–[3] in a first period. Furthermore, the notable evolution of ferrite loaded component technology made possible the development of transmission lines including ferrite substrate, particularly the microstrip line very suitable to be integrated in more complicated systems [4]. Some latter works were specially devoted to the theoretical analysis and understanding of the propagating modes in planar lines [5]–[8]. As a consequence of that, it was suggested how to build nonreciprocal components (phase shifters, isolators, circulator . . .) by using microstrips and slot-lines including magnetised ferrite substrates. From then on, the methods of analysis were increasing to make possible the study of a large class of multilayered planar lines with enhanced nonreciprocal behavior [9]–[17]. Different analytical or numerical methods were usually employed to treat these nonreciprocal structures: quasi-TEM approach [4], [7], modal expansion [6], [9], magnetic walls conditions [8], mode-matching [10], [13], [14], network analysis [11], singular integral equation approach [12] and the spectral domain technique [15]. This latter method has shown itself to be a widely used and very efficient scheme [18]–[27], suitable to be easily adapted to treat general planar structures when appropriate methods to determine the spectral dyadic Green's function (SDGF) are available. According to this, the application of the spectral domain approach requires the computation of the SDGF as a previous step. In this way, different approaches to compute the SDGF can be found in literature, from [21] which considers ferrite layers magnetised along a fixed transversal orientation, [19] applied to arbitrarily magnetised substrates up to [18], [28] capable to deal with complex bianisotropic media. The method developed by the authors in [28], namely the equivalent boundary method (EBM), provides some relevant features such as its stationary and perturbative nature and its closed form in terms of a straightforward algorithm.

The aim of the present work is to combine the EBM with the spectral domain technique in order to systematically pose the eigenvalue dispersive equation of a large class of planar transmission lines via the application of the Galerkin moment method in conjunction with an adequate choice of the base of functions. The method developed in this paper, that is the spectral domain-EBM (SD-EBM), makes it possible to study the propagation characteristics of strip-like/slot-like lines including coplanar multistrips/multislots embedded in a lossy bianisotropic multilayered linear medium. Special attention has been paid to all the numerical aspects concerning the employment of the SD-EBM. In this way, a study of the convergence of the method with the number of basis functions (for certain possible orientations of the magnetization) is presented, an adequate third-order asymptotic extraction of the SDGF is carried out, a suitable treatment of the tails involved is shown and an efficient method for searching zeros in the complex plane is discussed. This numerical treatment has been found very suitable to achieve reliable numerical data with tolerable CPU times, becoming specially adequate when the structure to be analysed involves very thin layers. The SD-EBM has been used in this work to analyse in detail a certain microstrip configuration and, as an example, the propagation characteristics of three asymmetric strips embedded in a four-layer medium involving a ferrite-semiconductor magnetised.

Manuscript received August 11, 1991; revised January 6, 1992. This work was supported by CICYT, Spain (Project No. TIC91-1018).

The authors are with the Universidad de Sevilla, Facultad de Fisica, Departamento de Electronica y Electromagnetismo, 41012, Sevilla, Spain.

IEEE Log Number 9200849.

II. Method of Analysis

As is well-known, the dispersive relation of a coplanar transmission line involving strips/slots embedded in a multilayered bianisotropic medium (as that shown in Fig. 1) can be posed, in the spatial domain, in terms of certain determinantal equation arising from the application of Galerkin method to the following operator equation

$$\left.\begin{aligned} \boldsymbol{E}_t(x) &= \mathcal{G}\boldsymbol{J}_t = \int_\Omega \mathcal{G}(x - x') \cdot \boldsymbol{J}_t(x')\, dx' \\ &\qquad \text{on the strips} \\ \boldsymbol{J}_t(x) &= \mathcal{L}\boldsymbol{E}_t = \int_\Omega \mathcal{L}(x - x') \cdot \boldsymbol{E}_t(x')\, dx' \\ &\qquad \text{in the slots} \end{aligned}\right\} \quad (1)$$

subjected to the corresponding boundary conditions on the strips/slots. Equation (1) has been posed making use of the dyadic Green's operator, $\mathcal{G}$, and the inverse of the dyadic Green's operator $\mathcal{L}$, $\boldsymbol{J}_t$, $\boldsymbol{E}_t$ being the tangential, (x, z), components of the current density and the electric field respectively. A dependence of the type $\exp j(-k_z z + \omega t)$ will be assumed but not written in all the quantities involved in the present analysis (k_z, stands for the complex propagation constant and ω for the angular frequency).

As previously established, the spectral domain analysis (SDA) applied to the computation of the propagation characteristics of planar transmission lines, namely to solving (1), via

$$\tilde{f}(k_x) = \frac{1}{2\pi}\int_{-\infty}^{\infty} f(x) \exp(jk_x x)\, dx, \quad (2)$$

has shown to be very efficient owing basically to two facts. Firstly, the SDA makes it possible to turn convolutional products into algebraic products and secondly, different methods to compute the SDGF, $\bar{\boldsymbol{G}}$, have been reported in literature. The authors have developed a different approach, namely the EBM, to compute numerically the SDGF in [28] based on the *Equivalence* and *Uniqueness* electromagnetic theorems. This method makes use of a (4×4) matrix formulation to obtain the electromagnetic vector, $\boldsymbol{X}_i = [\tilde{E}_{x,i}\ \tilde{E}_{z,i}\ \tilde{H}_{x,i}\ \tilde{H}_{z,i}]^T$, inside each layer in terms of

$$\boldsymbol{X}_i(y) = \exp(j\omega[\boldsymbol{Q}]_i y) \cdot \boldsymbol{X}_{o,i}, \quad (3)$$

$\boldsymbol{X}_{o,i}$ being a constant vector to be determined according to the boundary conditions, $[\boldsymbol{Q}]_i$ a matrix defined in [28] and related to the characteristics of the ith layer and $\exp(j\omega[\boldsymbol{Q}]_i y)$ a (4×4) matrix which can be related to the eigenvalues and eigenvectors of $[\boldsymbol{Q}]_i$.

Once (3) is posed for all the layers, the inverse of the SDGF, $\bar{\boldsymbol{L}}(k_x, k_z, \omega)$, rather than the SDGF, $\bar{\boldsymbol{G}}(k_x, k_z, \omega)$, is made up (taking into account the aforementioned electromagnetic theorem) by means of certain *stationary* (2×2) $[\boldsymbol{g}]_{i,j}$ matrices. These $[\boldsymbol{g}]_{i,j}$ matrices are built in such a way that they only relate quantities inside the ith layer, when certain *equivalent boundary conditions* are imposed to this layer. These *equivalent boundary conditions* make it possible to form the $\bar{\boldsymbol{L}}$ dyadic by linking simpler matrices. Each of these simpler matrices is related only to a single layer whose two surface fields are fixed. In this sense the EBM differs from other methods which link matrices related to layers whose surface fields are free. The fixed nature of the surface boundary conditions on each layer implies that the $\bar{\boldsymbol{L}}$ dyadic is built by means of stationary (rather than propagating) waves in the direction normal to the interfaces. The way of linking the $[\boldsymbol{g}]_{i,j}$ matrices to form the $\bar{\boldsymbol{L}}$ dyadic is shown in [28], where a systematic and general algorithm (including several internal metallized interfaces) is presented. This algorithm shows a well-conditioned numerical behavior and a perturbative nature arising from the decomposition inside each layer in stationary waves along the y-direction. The perturbative nature of the method basically accounts for the greatest importance of the layers closer to the internal metallization. This fact causes the EBM to be rather numerically insensitive to the increase of the number of layers and also it makes possible a direct knowledge of the asymptotic behavior of the SDGF [28] and its asymptotic equivalent structure. As a consequence of this, the feasibility to be generalized, the well-conditioned numerical behavior and the perturbative nature of the EBM make this method very suitable to be implemented by computer.

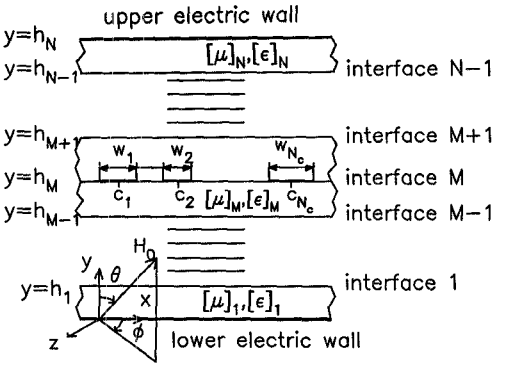

Fig. 1. Strip-like coplanar transmission line embedded in a bianisotropic multilayered medium. The slot-like line can be viewed by inverting the roles played by the metal and the interface on the internal metallized interface.

Once the $\bar{\boldsymbol{G}}$ or $\bar{\boldsymbol{L}}$ dyadics have been computed following [28] and taking into account that the presence of a single internal metallized interfaces makes that these dyadics are given by

$$\bar{\boldsymbol{L}}(k_x, k_z, \omega) = L_{xx}\boldsymbol{a}_x\boldsymbol{a}_x + L_{xz}\boldsymbol{a}_x\boldsymbol{a}_z + L_{zx}\boldsymbol{a}_z\boldsymbol{a}_x + L_{zz}\boldsymbol{a}_z\boldsymbol{a}_z \quad (4)$$

$$\bar{\boldsymbol{G}}(k_x, k_z, \omega) = G_{xx}\boldsymbol{a}_x\boldsymbol{a}_x + G_{xz}\boldsymbol{a}_x\boldsymbol{a}_z + G_{zx}\boldsymbol{a}_z\boldsymbol{a}_x + G_{zz}\boldsymbol{a}_z\boldsymbol{a}_z, \quad (5)$$

(1) can be rewritten, making use of the convolution and Parseval theorems, as

$$\left.\begin{aligned} \tilde{\boldsymbol{E}}_t(k_x) &= \bar{\boldsymbol{G}}(k_x, k_z, \omega) \cdot \tilde{\boldsymbol{J}}_t(k_x) \quad \text{on the strips} \\ \boldsymbol{J}_t(k_x) &= \bar{\boldsymbol{L}}(k_x, k_z, \omega) \cdot \tilde{\boldsymbol{E}}_t(k_x) \quad \text{in the slots} \end{aligned}\right\}. \quad (6)$$

The Galerkin method can be now applied to solve the above equations via an adequate finite expansion on the

unknown quantities taking into account the edge condition in the spatial domain, that is,

$$\tilde{\boldsymbol{J}}_t = \sum_{p=1}^{N_s}\sum_{n=0}^{N_f} c_{p,n}\tilde{\boldsymbol{J}}_{t,n}^{p} = \begin{Bmatrix}\tilde{J}_x \\ \tilde{J}_z\end{Bmatrix} = \begin{Bmatrix} \sum_{q=1}^{N_s}\sum_{m=0}^{N_{f-1}} a_{q,m} J_{x,m}^{q} \\ \sum_{p=1}^{N_s}\sum_{n=0}^{N_f} b_{p,n} J_{z,n}^{p}\end{Bmatrix} \quad \text{on the strips} \tag{7}$$

$$\tilde{\boldsymbol{E}}_t = \sum_{p=1}^{N_s}\sum_{n=0}^{N_f} c_{p,n}\tilde{\boldsymbol{E}}_{t,n}^{p} = \begin{Bmatrix}\tilde{E}_x \\ \tilde{E}_z\end{Bmatrix} = \begin{Bmatrix} \sum_{p=1}^{N_s}\sum_{n=0}^{N_f} a_{p,n} E_{x}^{p,n} \\ \sum_{q=1}^{N_s}\sum_{m=0}^{N_{f-1}} b_{q,m} E_{z,m}^{q}\end{Bmatrix} \quad \text{in the slots} \tag{8}$$

with the indices p, q standing for the order of the strips/slots indistinctly, the index n for the order of the expansion in each strip/slot, N_s for the total number of strips/slots and N_f for the higher order of the basis function in the expansion. This expansion is made using the first and second kind of the Chebychev polynomial [29] (weighted by the proper function to account for the edge condition) whose spectral transformed are found to be

$$\begin{Bmatrix}\tilde{J}_{z,n}^{p} \\ \tilde{E}_{x,n}^{p}\end{Bmatrix} = j^{n} J_n\left(\frac{\omega_p}{2} k_x\right) \exp\left(jk_x c_p\right) \tag{9}$$

$$\begin{Bmatrix}\tilde{J}_{x\,x,m}^{p} \\ \tilde{E}_{z}^{q,m}\end{Bmatrix} = j^{m+1}\pi(m+1)\frac{J_{m+1}\left(\frac{\omega_q}{2} k_x\right)}{k_x} \exp\left(jk_x c_q\right) \tag{10}$$

($J_n(\cdot)$ stands for the Bessel function of first kind and nth order).

The application of the Galerkin moment method to (6), when the boundary condition (1) is imposed to each basis function, gives rise to the following indeterminate systems of equations

$$\sum_{p=1}^{N_s}\sum_{n=0}^{N_f} c_{p,n}\int_{-\infty}^{\infty} (\tilde{\boldsymbol{J}}_{t,m}^{p}(k_x))^{*} \cdot \overline{\boldsymbol{G}}(k_x, k_z, \omega) \cdot \tilde{\boldsymbol{J}}_{t,n}^{p}(k_x)\, dk_x = 0 \quad \text{on the strips} \tag{11}$$

$$\sum_{p=1}^{N_s}\sum_{n=0}^{N_f} c_{p,n}\int_{-\infty}^{\infty} (\tilde{\boldsymbol{E}}_{t,m}^{q}(k_x))^{*} \cdot \overline{\boldsymbol{L}}(k_x, k_z, \omega) \cdot \tilde{\boldsymbol{E}}_{t,n}^{p}(k_x)\, dk_x = 0 \quad \text{in the slots.} \tag{12}$$

Each one of the above system of equations can be rewritten in matrical form as

$$[\boldsymbol{\Gamma}(k_z, \omega)] \cdot \boldsymbol{c} = 0, \tag{13}$$

$[\boldsymbol{\Gamma}]$ being a squared matrix of $N_s \cdot (2N_f + 1)$ dimension. The equation (13) can be viewed as an eigenvalue problem in case the value of ω is fixed. In this sense, the dispersive equation of the structure can be posed as

$$\det\,[\boldsymbol{\Gamma}(k_z, \omega)] = 0, \tag{14}$$

whose complex solutions $k_{z,\nu}$ ($\nu = 1, \cdots, N_{\text{modes}}$), namely the different eigenvalues of (13), account for the complex propagation constant of each mode and the entries of corresponding eigenvector $\boldsymbol{c}_{\nu}$ are the different coefficients of the expansion of $\tilde{\boldsymbol{J}}_t$ or $\tilde{\boldsymbol{E}}_t$.

III. Numerical Aspects

Once the eigenvalue problem (13) has been posed, two main numerical problems arise: a) the numerical computation of the integrals involved in (11) or (12) and b) the searching for the complex eigenvalues in (14). Since the numerical problems related to the strip-like and the slot-like problems are very similar, only the strip-like problem will be considered henceforth.

Note that all the integrals appearing in (11) have the following general form (apart from constants):

$$\Gamma_{\alpha\beta}^{pnqm} = \int_{-\infty}^{\infty} J_n\left(\frac{\omega_p}{2} k_x\right) G_{\alpha\beta}(k_x, k_z, \omega) \cdot J_m\left(\frac{\omega_q}{2} k_x\right) e^{j(c_p - c_q)k_x}\, dk_x \tag{15}$$

(α, β stand indistinctly for x or z). The procedure followed to treat the numerical integration of (15) basically resides on certain decomposition in conjunction with an appropriate asymptotic scheme. Thus, the $\Gamma_{\alpha\beta}^{pnqm}$ coefficients can be written as:

$$\begin{aligned}\Gamma_{\alpha\beta}^{pnqm} = {} & \int_{-u}^{u} J_n\left(\frac{\omega_p}{2} k_x\right) G_{\alpha\beta}(k_x, k_z, \omega) J_m\left(\frac{\omega_q}{2} k_x\right) e^{j(c_p - c_q)k_x}\, dk_x + \int_{u}^{\infty} J_n\left(\frac{\omega_p}{2} k_x\right)[G_{\alpha\beta}(k_x, k_z, \omega) \\ & - G_{\alpha\beta}^{\infty}(k_x)] J_m\left(\frac{\omega_q}{2} k_x\right) e^{j(c_p - c_q)k_x}\, dk_x + \int_{-\infty}^{-u} J_n\left(\frac{\omega_p}{2} k_x\right)[G_{\alpha\beta}(k_x, k_z, \omega) - G_{\alpha\beta}^{-\infty}(k_x)] J_m\left(\frac{\omega_q}{2} k_x\right) e^{j(c_p - c_q)k_x}\, dk_x \\ & + \int_{u}^{\infty} J_n\left(\frac{\omega_p}{2} k_x\right) G_{\alpha\beta}^{\infty}(k_x) J_m\left(\frac{\omega_q}{2} k_x\right) e^{j(c_p - c_q)k_x}\, dk_x + \int_{-\infty}^{-u} J_n\left(\frac{\omega_p}{2} k_x\right) G_{\alpha\beta}^{-\infty}(k_x) J_m\left(\frac{\omega_q}{2} k_x\right) e^{j(c_p - c_q)k_x}\, dk_x \end{aligned} \tag{16}$$

with $G^{\infty}_{\alpha\beta}(k_x)$ and $G^{-\infty}_{\alpha\beta}(k_x)$ being the asymptotic functions (not depending on k_z and ω) of $G_{\alpha\beta}(k_x, k_z, \omega)$ when the spectral variable, k_x, tends to ∞ and $-\infty$ respectively. The integration limit u is chosen in such a way that the relative error between $G_{\alpha\beta}(k_x, k_z, \omega)$ and its corresponding asymptotic function is small (usually 10%). It should be noticed that the particular scheme employed in the numerical integration of (16) has been carried out principally to compute the SDGF as few times as possible. This fact can become very relevant since the computational effort required to obtain the SDGF is usually much greater than that necessary to compute the Bessel functions. In this way, it has been found, after comparing with other possible schemes, that (16) turns out to be an optimum way to compute numerically the integrals involved.

The first term of expression (16) is a definite integral and therefore this term can be successfully integrated by using a numerical procedure based on Gauss-Legendre quadratures and checking that the result is not affected when the order of the quadrature is increased. The second and third terms of (16) are integrals with infinite limits of integration but they are calculated following an iterative application of the numerical method employed for the first term. Nevertheless, since $[G_{\alpha\beta}(k_x, k_z, \omega) - G^{\pm\infty}_{\alpha\beta}(k_x)]$ tends fast to zero (as will be shown in the next section), these integrals are rapidly convergent. The fourth and fifth terms, that is the tails, are computed following a different scheme to be explained later.

As has been mentioned above, the feasibility of the proposed method requires to achieve an adequate asymptotic behavior of $G_{\alpha\beta}(k_x, k_z, \omega)$. The perturbative nature of the EBM makes it straightforward to predict the asymptotic behavior [28], [30] which can be written as:

$$G^{\pm\infty}_{xx}(\pm k_x) = A^{\pm}_{xx} \cdot (\pm k_x) + B^{\pm}_{xx} + \frac{C^{\pm}_{xx}}{\pm k_x} + \cdots \quad (17)$$

$$G^{\pm\infty}_{xz}(\pm k_x) = A^{\pm}_{xz} + \frac{B^{\pm}_{xz}}{\pm k_x} + \frac{C^{\pm}_{xz}}{(\pm k_x)^2} + \cdots \quad (18)$$

$$G^{\pm\infty}_{zx}(\pm k_x) = A^{\pm}_{zx} + \frac{B^{\pm}_{zx}}{\pm k_x} + \frac{C^{\pm}_{zx}}{(\pm k_x)^2} + \cdots \quad (19)$$

$$G^{\pm\infty}_{zz}(\pm k_x) = \frac{A^{\pm}_{zz}}{\pm k_x} + \frac{B^{\pm}_{zz}}{(\pm k_x)^2} + \frac{C^{\pm}_{zz}}{(\pm k_x)^3} + \cdots . \quad (20)$$

Note that different asymptotic behaviors have been assumed when the spectral variable tends either to minus infinity or to plus infinity. This distinction has been made to account for the most general form of the SDGF. In this work, an asymptotic behavior of *third order* for each element in the $G^{\pm\infty}_{\alpha,\beta}(\pm k_x)$ dyadic is retained since this behavior would imply to obtain the second and third integral in (16) (assuming that the $\pm\infty$ integration limits are fixed to suitable finite values) with three significant digits more than in case a simpler asymptotic behavior of first order was employed. Unfortunately, there are only a few simple cases in which it is possible to find an accessible analytical procedure for determining all the constants involved in expressions (17)–(20) [30]. Nevertheless, the three constants appearing in the asymptotic expansion of $G^{\pm\infty}_{\alpha,\beta}(k_x)$ can be obtained in terms of three values of these functions which correspond to three different larger values of $\pm k_x(\pm k_{x,1}, \pm k_{x,2}, \pm k_{x,3})$. As an example, the following system of three equations is found for the G^{∞}_{xx} case:

$$\left.A^{+}_{xx} \cdot (k_{x,i}) + B^{+}_{xx} + \frac{C^{+}_{xx}}{k_{x,i}} = G^{\infty}_{xx}(k_{x,i}) \qquad i = 1, 2, 3\right\}. \quad (21)$$

The integrals concerning the fourth and fifth terms of expression (16) turn out to have the following general form (apart from the corresponding constants)

$$K^{\pm}_{pnqm,i} = (\pm 1)^{n+m-i} \int_u^{\infty} \frac{J_n\left(\frac{\omega_p}{2} k_x\right) J_m\left(\frac{\omega_q}{2} k_x\right)}{(k_x)^i} \cdot e^{\pm j(c_p - c_q)k_x}\, dk_x \quad (22)$$

($i = 1, 2, 3$). Different treatment is applied to expression (22) in Appendix depending if (22) refers to interaction between two different ($p \neq q$) or equal strips ($p = q$). The analysis shown in the Appendix provides accurate numerical values of the above integrals with a reduced computational effort.

As far as the numerical treatment has been developed at this section, the appearance of singularities along the integration path of (16) has been neglected. As is well known, these singularities stem from the real poles appearing in the SDGF of a lossless transmission line. These poles account for the propagation constants of the different modes in the lossless parallel-plate waveguide which supports the transmission line and are related to the appearence of leaky waves in the line. An appropiate treatment of this topic can be found in [31] (in case the wave propagation has an isotropic nature) where it is also suggested a procedure to overcome the appearance of singularities in the numerical integration. Unfortunately the treatment to solve this drawback requires the previous knowledge of the propagation constants in the parallel-plate waveguide. This knowledge can be straightforward in the simplest isotropic dielectric case but gets complicated in the case of substrate with magnetised ferrite. The magnetised ferrite-loaded waveguides show on one hand a more involved modal spectrum and on the other hand, it is necessary to investigate the propagation along all the directions in the $(x - z)$ plane owing to the strong anisotropy shown by the wave propagation in this plane. An efficient approach to compute the propagation constant in these structures have been recently developed by the authors in [32]. Apart from the above procedure, the drawbacks in the integration are often avoided by inserting losses in the substrates. The present work is not concerned with the investigation of leaky waves and therefore only the non-radiating zone of the modal spectrum of the transmission line is taken into account. Future works

should be devoted to the investigation of leaky waves in ferrite-loaded transmission lines.

Once the matrix $[\Gamma(k_z, \omega)]$ has been built up, another numerical problem appears relating to the searching for the complex eigenvalues of (13), namely the zeros of (14). Now, the most important task is to find an efficient method to systematically analyse the complex plane. In this way, the integral method C) described in [33] has been found to be very suitable for this purpose when the function $F(k_z) = \det [\Gamma(k_z, \omega_{\text{fixed}})]$ is assumed to be analytic in the region of searching. This method makes possible a previous examination of a circular region in order to determine the existence of zeros. If the existence of ν zeros has been predicted, these zeros turn out to be the roots of a νth degree polinomial. The main drawback of the method could be the inability to deal with meromorphic functions, nevertheless the zone in which $F(k_z)$ becomes meromorphic coincides with the radiating modal zone of the line (which is not treated in this work as has previously been mentioned).

IV. Numerical Results

At this section, all the numerical aspects concerning the application of the method exposed above are checked and discussed. As an example, a lossless microstrip with a superstrate of magnetised ferrite, as studied in [26], has been chosen to carry out the numerical discussion. First of all, the elements of the SDGF (k_z and ω fixed) for this structure are plotted in Fig. 2(a)–(c) where three different magnetizations (parallel to the three main axis) are considered (notice that in Fig. 2(a) the three cases are superimposed). It can be seen from these three figures that the behavior of $G_{\alpha,\beta}(k_x, k_z, \omega)$ for large values of the spectral variable coincides with that predicted by expressions (17)–(20). If each magnetization is studied separately it is observed that in case the magnetization is parallel to the x-axis, $\boldsymbol{H}_0 = H_0 \boldsymbol{a}_x$, the different elements of the SDGF have a well defined symmetry, that is, Im G_{xx} and Im G_{zz} are even functions of k_x and Im G_{xz} is an odd one (real parts are null). In case the magnetization is assumed to be parallel to the y-axis, the same behavior as that of the above case is observed. Note that G_{xz} presents now real even part distinct to zero. All these properties numerically observed can be easily obtained from the application of the reciprocity theorem and/or simple symmetry reasonings [32]. If the magnetization is parallel to the z-axis, there are not any symmetry respect to the spectral variable. Im G_{xx} and Im G_{xz} have weak nonsymmetry (almost imperceptible in the figures), on the contrary Im G_{zz} presents a very strong nonsymmetry, more relevant if the operation frequency is within the zone of *forbidden frequency* [34]. The strong nonsymmetry of the *spectral zz*-component of the Green's dyadic makes the corresponding spatial component of this dyadic a complex function with different behavior in the real and imaginary parts. Hence, the phase of this complex function shows an involved dependence with the spatial variable, x. The involved behavior or this spatial complex component in

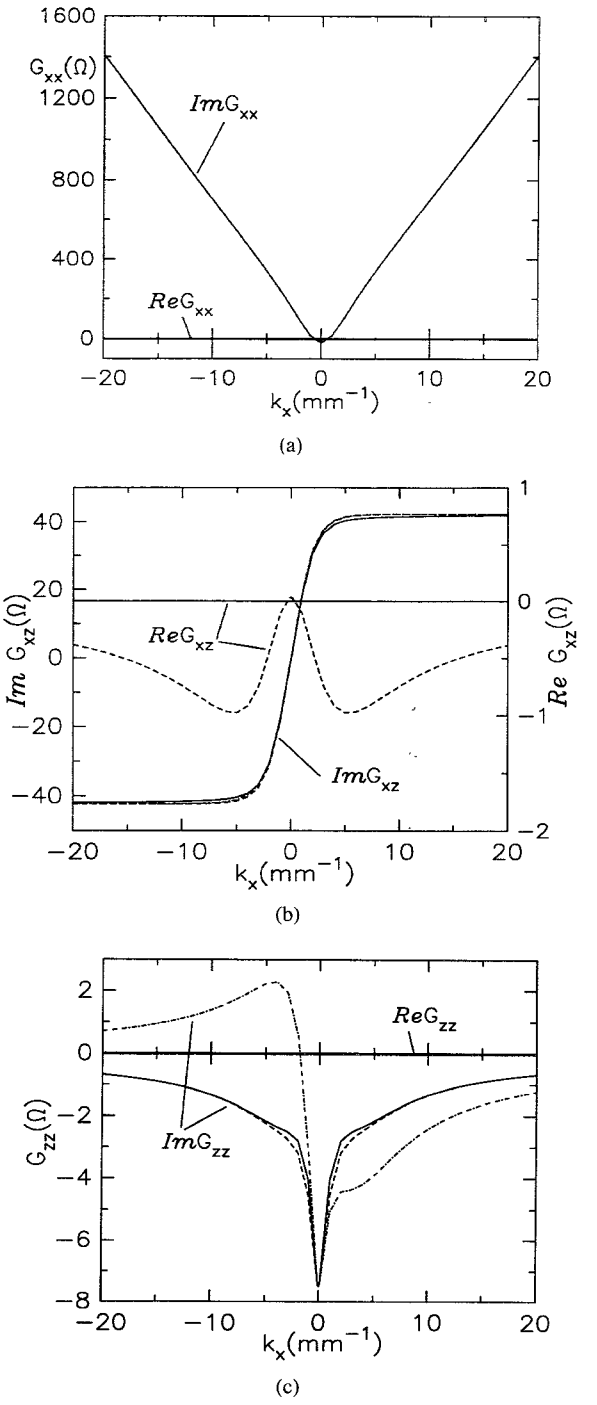

Fig. 2. Behavior of the different elements of the SDGF: (a) $-G_{xx}$, (b) $-G_{xz}$ and (c) $-G_{zz}$ for different magnetizations in a microstrip with a ferrite-superstrate with the following characteristics: $h_1 = 0.254$ mm., $h_2 = 0.254$ mm., $h_3 = 2$ mm., $\epsilon_1 = 12.9$, $\mu_1 = 1$, $\epsilon_2 = 12.6$, $4\pi M_s = 2750$ G., $H_0 = 275$ Oe., $\epsilon_3 = \mu_3 = 1$, $\omega_1 = 1.016$ mm., $k_z = 0.3$ mm^{-1}, Freq = 10 GHz. (——): $\boldsymbol{H}_0 = H_0 \boldsymbol{a}_x$, (- - - - - - -): $\boldsymbol{H}_0 = H_0 \boldsymbol{a}_y$, (-·-·-·—·—·—): $\boldsymbol{H}_0 = H_0 \boldsymbol{a}_z$.

conjunction with the requirement of $\boldsymbol{E}_t = 0$ on the strip causes the resulting current density $\boldsymbol{J}_t$ to be complex and to have an involved behavior. This behavior should be simulated in the *finite space* provided by the basis functions. The space of functions chosen to solve the dispersion equation was formed by the first and second kind of Chebyshev polynomials, which means that each dimen-

sion of this space is made up by an odd/even function. According to this, it should be rather difficult to form the nonsymmetric current density in this space of functions with a reasonable number of basis functions. The nonsymmetry of the current density can be also explained from physical arguments if it is noticed that there is an important power flux along the x-direction in the parallel-plate waveguide which supports the transmission line [32]. The perturbation imposed by the strips prevents the appearence of x-directed power flux but it should imply strongly nonsymmetric current density, in other words, edge-modes [8].

Another relevant numerical fact related to the SDGF to be discussed is the convenience of using an asymptotic behavior of third order. It was suggested at the previous section that this choice made the involved integrals accurately computed. This fact can now be understood if it is noted of Fig. 3(a)–(c) that the relative error $\Delta G_{\alpha,\beta} = (|G_{\alpha,\beta} - G_{\alpha,\beta}^{\pm\infty}|/|G_{\alpha,\beta}|)$ related to the use of a third-order asymptotic curve-fitting is approximately three orders of magnitude minor than that related to the first-order asymptotic extraction. The use of a third-order asymptotic curve-fitting implies to determine the constants appearing in (17)–(20) and compute the tails shown in the appendix. This computational effort is completely justified by the important saving of CPU-time and the accuracy in the obtaining of the second and third terms of (16). Extractions of higher order (which implies more involved analytical preprocessing and numerical effort to compute the tails) could be made if a very extreme accuracy is desired.

Next, the convergence of the propagation constant with the number of basis functions is analysed. The evolution of the normalised phase constant β/β_0 is shown in Fig. 4 when the angle of magnetization is varied in the $(x - z)$ plane and the frequency is fixed out of the zone of forbidden frequencies in the aforementioned microstrip with a ferrite-superstrate. It is noted of this figure that our numerical results differ from those provided by [26] in proportion to the increase of the number of basis functions, N_f (the total number of basis functions is $2N_f + 1$), nevertheless the discrepancy never goes beyond 1.5%. A detailed study of the convergence when different magnetizations are considered can be found in Table I. This table shows the good convergence appearing in case the magnetization is contained in the $(x - y)$ plane ($\phi = 90°$, $\theta = 0°, 30°, 60°, 90°$). Just five basis functions are required to achieve a definitive convergence in this case. The convergence gets a bit worse as far as the projection of the magnetization in the z-axis becomes larger. Thus, it is observed that for $\theta = 90°$, $\phi = 60°$, $90°$ and $\phi = 90°$, $\theta = 60°$ the fifth significant digit is not assured with 17 basis functions. With regard to the less good convergence shown by the phase constant in the above case, it should be interesting to investigate the evolution of the normalized current density when the number of basis functions is increased. The current density will be normalized henceforth by making that the coefficient of higher modulus in the current density expansion is set to unity. This evolution is plotted in Fig. 5(a)–(b) for $J_x^{\text{norm.}}$ and $J_z^{\text{norm.}}$ respectively showing on the one hand certain poor convergence and on the other hand the predicted complex nature of these quantities. It should be noticed the opposite parity of the real and the imaginary part of both $J_x^{\text{norm.}}$ and $J_z^{\text{norm.}}$. This fact implies that the phase of both components of current varies continuously and strongly along the strip section. This strong dependence suggestes that the current wavefronts below the strip are

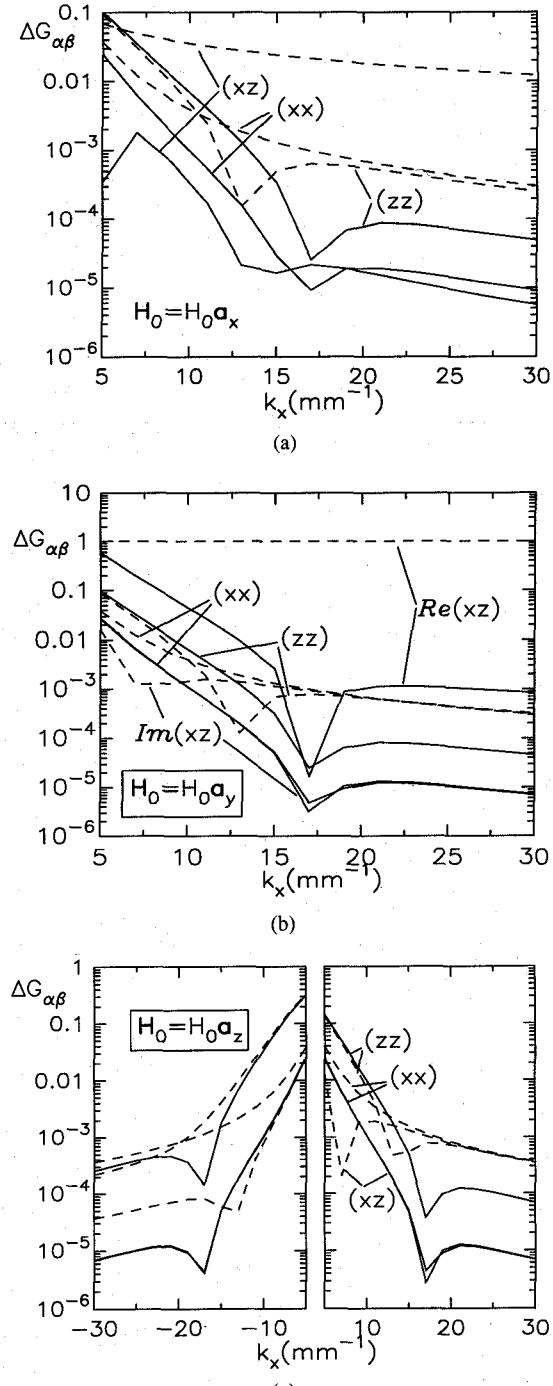

Fig. 3. Relative error of the different elements of the SDGF with magnetizations along the main axis: (a): $\boldsymbol{H}_0 = H_0\boldsymbol{a}_x$, (b): $\boldsymbol{H}_0 = H_0\boldsymbol{a}_y$ and (c): $\boldsymbol{H}_0 = H_0\boldsymbol{a}_z$ for the configuration of Fig. 2 when either a first-order: (- - - - - - -) or a third-order: (———) asymptotic behaviors are used.

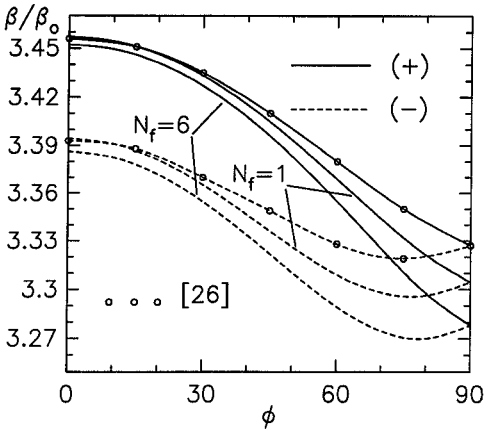

Fig. 4. Normalized plane constant when the magnetization is varied in the $(x - z)$ plane ($\theta = 90°$) for the same configuration of Fig. 2.

TABLE I
CONVERGENCE OF THE NORMALIZED PHASE CONSTANT WITH THE NUMBER OF BASIS FUNCTIONS FOR SEVERAL ARBITRARILY ORIENTED MAGNETIZATIONS IN THE CONFIGURATION ANALIZED IN FIG. 2 (FREQ = 10 GHz)

	$\theta = 90°$			
N_f	$\phi = 0°$	$\phi = 30°$	$\phi = 60°$	$\phi = 90°$
0	3.39449	3.37047	3.32535	3.32229
1	3.39449	3.36547	3.30906	3.30447
2	3.38634	3.35677	3.29913	3.29721
3	3.38634	3.35525	3.29265	3.28537
4	3.38634	3.35516	3.29072	3.28057
5	3.38634	3.35490	3.29013	3.27993
6	3.38634	3.35486	3.28942	3.27801
7	3.38634	3.35477	3.28929	3.27798
8	3.38634	3.35474	3.28895	3.27713

	$\phi = 0°$			$\phi = 90°$	
N_f	$\theta = 0°$	$\theta = 30°$	$\theta = 60°$	$\theta = 30°$	$\theta = 60°$
0	3.43337	3.41687	3.40127	3.41016	3.35519
1	3.43337	3.41687	3.40127	3.40748	3.34412
2	3.42724	3.40987	3.39345	3.40174	3.33811
3	3.42724	3.40987	3.39345	3.40003	3.33084
4	3.42724	3.40987	3.39345	3.40001	3.32939
5	3.42724	3.40987	3.39345	3.39969	3.32854
6	3.42724	3.40987	3.39345	3.39966	3.32786
7	3.42724	3.40987	3.39345	3.39955	3.32767
8	3.42724	3.40987	3.39345	3.39953	3.32733

not perpendicular to the direction of propagation, not even approximately. This fact is in accordance with the presence of spectral components of the field carrying a nonzero power in a direction parallel to theirs wavefronts. Other studies have been carried out for the cases denoted above as good convergent ones and it has been found that the degree of good convergence shown by the phase constant is reflected in the current density. The case pointed out in this work as the most problematic one (namely the configuration under study when the magnetization is along the z-axis and the operation frequency is within the forbidden frequency zone) has been treated in [24]. The authors of that work seem not to be aware of some numerical problem related to this critical case and suggest a sufficiently good convergence in the propagation parameters just with 9 basis functions. A study of the convergence concerning the phase constant of the configuration treated in Fig. 5 of [24] is shown in Table II for two values of frequency. It has been found an acceptable convergence in case the frequency is 3.2 GHz but no convergence has been detected up to 17 basis functions in case frequency is 4.5 GHz (we have found that this fact is not related to the appearance of poles close to the k_x-axis of integration). This apparent null convergence is also observed in the current density plotted in Fig. 6. The curves of this figure show that the increasing in the number of basis functions from 15 to 17 has a drastic effect on the behavior of the current density. This fact suggestes that the convergence is still far from being achieved. Thus, the Chebyshev-type basis functions do not seem to be the most adequate to deal with this particular case. Future works should be devoted to a deeper investigation on this subject.

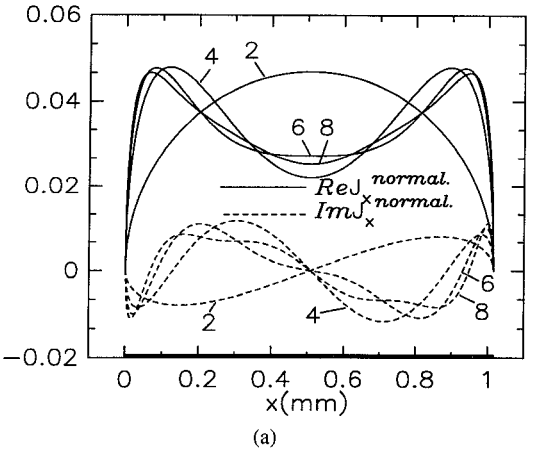

(a)

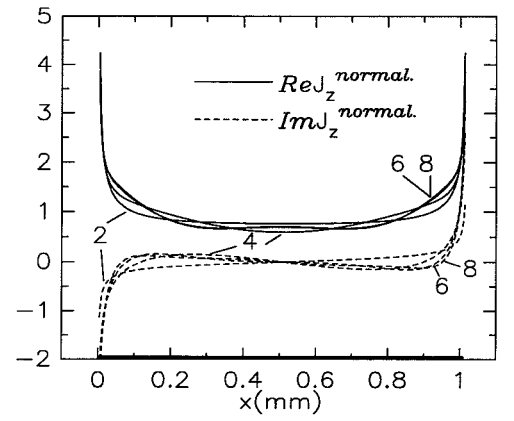

(b)

Fig. 5. Convergence of the components of the current density on the strip (a): $J_x^{\text{norm}}(x)$ and (b): $J_z^{\text{norm}}(x)$ with the number of basis functions. The same configuration of Fig. 2 is considered with Freq = 10 GHz., $\boldsymbol{H}_0 = H_0 \boldsymbol{a}_z$.

In the following we restrict ourselves to analyse configurations in which the convergence has been properly checked. In this way, the configuration treated in [26] with magnetization parallel to the x-axis is now analysed in the range of forbidden frequencies. The modal spectrum in

TABLE II
CONVERGENCE OF THE NORMALIZED PHASE CONSTANT WITH THE NUMBER OF BASIS FUNCTIONS FOR A MICROSTRIP LONGITUDINALLY MAGNETIZED: $h_1 = 1.27$ mm., $\epsilon_1 = 17.5$, $4\pi M_s = 2267$ G., $\boldsymbol{H}_0 = (144 \text{ Oe})\boldsymbol{a}_z$, $\Delta H_0 = 300$ Oe., $h_2 = 2.03$ mm., $\epsilon_2 = 10.2$, $h_3 = 20$ mm., $\epsilon_3 = 1$, $\omega = 0.3$ mm ((**) DATA EXTRACTED FROM FIG. 5 OF [24])

	k_z (mm^{-1})	
N	Freq = 3.2 GHz	Freq = 4.5 GHz
0	(0.37142 − *j*0.13555)	(0.19444 − *j*0.13187)
1	(0.36142 − *j*0.11007)	(0.34226 − *j*0.14754)
2	(0.36339 − *j*0.10452)	(0.22671 − *j*0.18021)
3	(0.36306 − *j*0.10533)	(0.31038 − *j*0.14844)
4	(0.36282 − *j*0.10423)	(0.24143 − *j*0.18897)
5	(0.36303 − *j*0.10447)	(0.29802 − *j*0.15083)
6	(0.36280 − *j*0.10417)	(0.24992 − *j*0.19137)
7	(0.36296 − *j*0.10428)	(0.29144 − *j*0.15286)
8	(0.36282 − *j*0.10412)	(0.25545 − *j*0.19187)
**	(0.36 − *j*0.11)	(0.22 − *j*0.18)

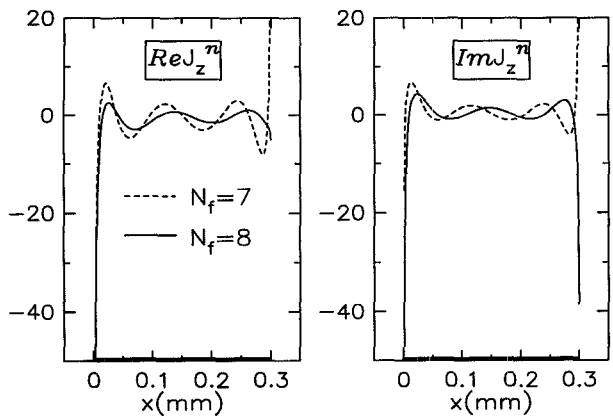

Fig. 6. Behavior of $J_z^{\text{norm}}(x)$ with different number of basis functions for the configuration of Table II with Freq = 4.5 GHz.

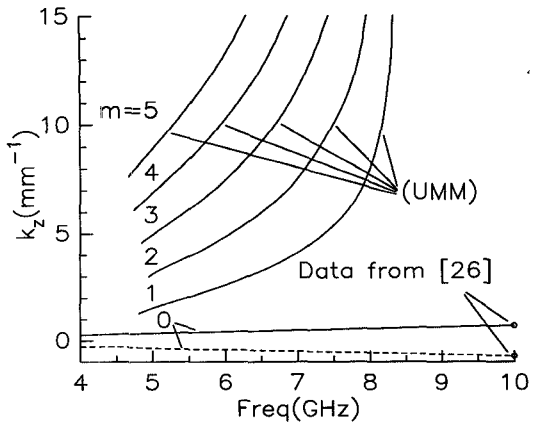

Fig. 7. Propagating modal spectrum for the configuration of Fig. 2 with $\boldsymbol{H}_0 = H_0\boldsymbol{a}_x$.

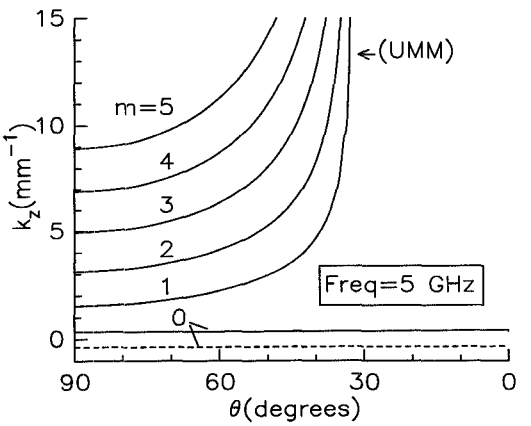

Fig. 8. Propagation constant of the modes reported in Fig. 7 as a function of the angle θ.

this zone is shown in Fig. 7. The typical electromagnetic mode ($m = 0$) appears in the lower zone showing certain nonreciprocity. In addition, five modes ($1 \leq m \leq 5$) are also found just in the positive zone of k_z with three relevant characteristics: a) they only appear propagating along the $+z$ direction, b) the phase constants of these modes are large and present asymptotic behaviors and c) these modes become radiating approximately below 4.9 GHz. According to characteristics a) and b), that is, the total nonreciprocity of these modes and a supposed magnetostatic nature, these modes have been denoted as Unidirectional Magnetostatic Modes (UMM).

Regarding characteristic c), it could seem surprising the fact that these modes radiate laterally whereas the electromagnetic mode does not radiate despite of having the smallest phase constant value. This apparent contradiction can be explained if the anisotropic nature of the wave propagation in the parallel-plate housing waveguide is taken into account. In fact, as is well known, radiation of leaky waves in strip-like structures occurs when a mode with propagation constant vector $\boldsymbol{k} = (k_x, k_z)$ (k_z being the propagation constant of the line) can be excited in the housing waveguide. If the housing waveguide has azimuthal symmetry, this means that radiation occurs for all k_z whose real part is less than the propagation constant, β, of the upper waveguide mode. However, if the housing waveguide has not azimuthal symmetry this rule is no longer valid. In this latter case, the existence of a propagating mode in the housing waveguide with propagation constant $\beta > k_z$ in a given direction, does not imply the existence of other waveguide modes with propagation constant (k_x, k_z); $\beta^2 = k_x^2 + k_z^2$, for *all* $k_z < \beta$ but only for certain k_z. The strong anisotropy of wave propagation in dielectric-ferrite-dielectric waveguides magnetised at an arbitrary direction in the $(x - z)$ plane is analyzed in [32].

The effect of the varying of the angle of magnetization in the $(x - y)$ plane for a fixed frequency is plotted in Fig. 8. The curves of this figure show how the electromagnetic mode is slightly affected by the angle of magnetization unlike what happens to the UMM's. The asymptotic behavior of these modes at certain intermediate angles of magnetization is somewhat expected since the microstrip turns out to be reciprocal in case the external magnetic biased field is oriented along the y-axis. This fact implies that the UMM's can not exist under this condition of reciprocity.

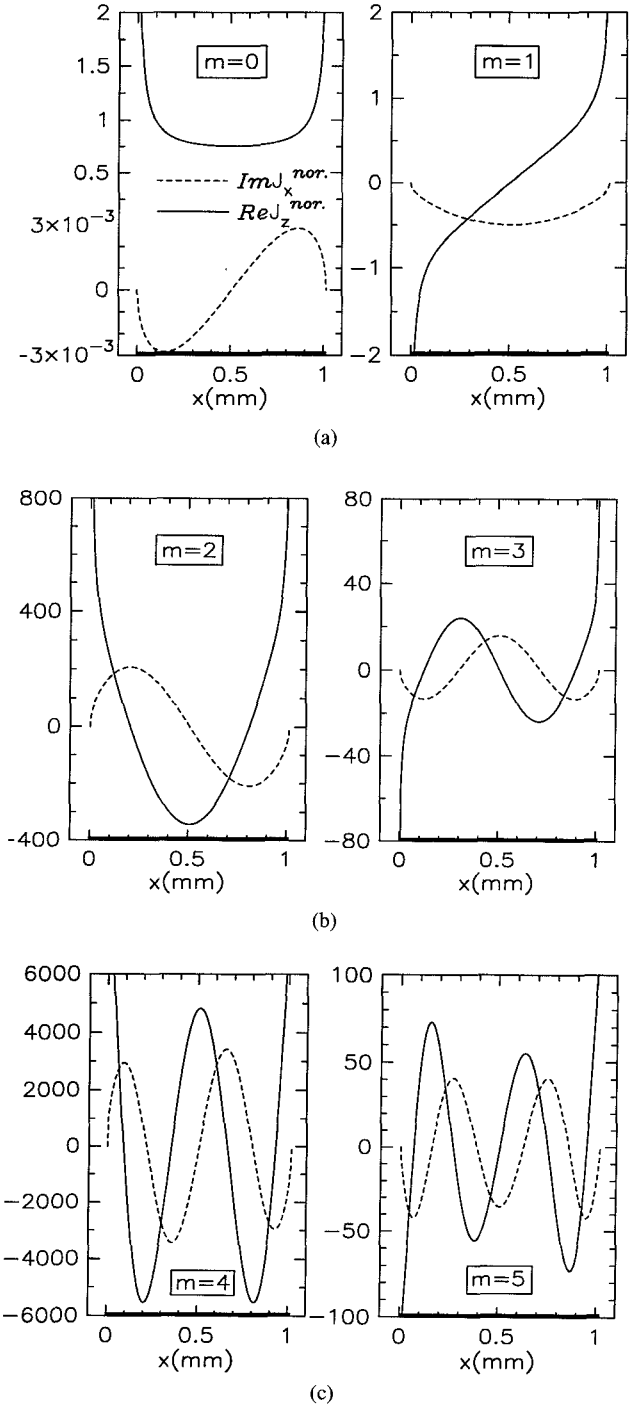

Fig. 9. (a)-(c): Behavior of the current density for the different modes shown in Fig. 7 with Freq = 5 GHz.

Valuable information about the nature of the modes can be extracted from Fig. 9(a)-(c) where the behavior of Im $J_x^{\text{norm.}}$ and Re $J_z^{\text{norm.}}$ in all these modes is shown (Re $J_x \equiv$ Im $J_z = 0$). Thus, two essential differences should be observed between the electromagnetic mode and the UMM's: a) $J_z^{\text{norm.}}$ is always positive for $m = 0$ and passes through zero in the other cases. b) $J_x^{\text{norm.}}$ is negative on the left side of the strip and positive on the right side for the electromagnetic mode, this behavior disappearing in

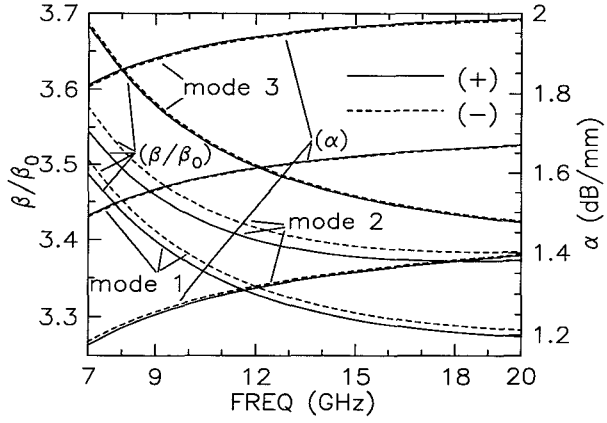

Fig. 10. Modal propagation parameters for the three fundamental modes in a transmission line with a gyrotropic-dielectric-semiconductor-air composite medium and three asymmetric strips above the second layer. h_1 = 200 μm., ϵ_1 = 12.9, $\boldsymbol{H}_0$ = (1000 Oers.) $\boldsymbol{a}_x$, $n = 10^{14}$ cm^{-3}, $\tau = 10^{-13}$ s., $4\pi M_s$ = 1600 G., h_2 = 100 μm., ϵ_2 = 12.6, h_3 = 100 μm., ϵ_3 = 12.3, σ_3 = 0.01 (Ω mm)$^{-1}$, h_4 = 1 mm., ϵ_4 = 1, c_1 = 50 μm., ω_1 = 100 μm., c_2 = 275 μm., ω_2 = 150 μm., c_3 = 600 μm., ω_3 = 200 μm.

the UMM's. These two differences suggest that the behavior of the current density on the strip is basically distinct in each type of mode, that is, whereas the electromagnetic mode presents similar current lines as those of a quasi-TEM mode, the UMM's seem to have these current lines making so many loops as the value of their index m indicates. If the current lines are making loops, this means that $\nabla \cdot \boldsymbol{J} \approx 0$ or analogously that $\nabla \times \boldsymbol{H} \approx \boldsymbol{J}$, expression which is in accordance with the predicted magnetostatic nature of the UMM's. In order to verify this assertion, numerical computations have been made showing that $\nabla \cdot \boldsymbol{J}$ for modes with $m \neq 0$ is at least two orders of magnitude less than $\nabla \cdot \boldsymbol{J}$ corresponding to the electromagnetic mode.

Up to now, just the magnetized ferrite-superstrate microstrip configuration has been analysed. The method developed in this work has been also applied to the study of more involved configurations. As an example Fig. 10 shows the propagation parameters as a function of frequency for the three fundamental modes appearing in a multilayered transmission line with three asymmetrical strips. The multilayered medium is composed by four layers, the first of them being a ferrite with nonnegligible conductivity magnetised along the x-axis (as a consequence of that, this layer acquires both gyromagnetic and gyroelectric characteristics), the second layer a dielectric, the third a semiconductor and the fourth air. A typical CPU time to achieve five significant digits in the three propagation parameters corresponding to the three modes (for a fixed frquency) has found to be 45 seconds in a CONVEX-220 machine. Apart from this configuration, certain nonreciprocal slow-wave lines involving asymmetrical strips or slots have been analysed by the authors in [35]. As is well known, the presence of very thin layers in these slow-wave lines makes that the integrals involved show an extremely slow convergence. Hence the numer-

ical scheme reported in this work turns out to be specially suitable in the analysis of these configurations, achieving accurate numerical results with tolerable CPU times.

V. Conclusion

This work presents an efficient numerical application of the Galerkin method in the spectral domain making use of the general algorithm for obtaining the SDGF in bianisotropic media provided by the EBM. Since in a great number of practical cases (such as those including several layers and/or gyroelectric/gyromagnetic characteristics) the most consuming CPU time is related to the numerous computations of the SDGF, the numerical scheme proposed in the present work has been chosen in order to optimize the number of times that the SDGF should be computed. This optimization has been achieved on the one hand by extracting a suitable asymptotic curve-fitting to the SDGF and on the other hand by taking advantage of certain numerical integration scheme. The asymptotic behavior of the SDGF is straigforwardly predicted by the EBM, the constants related to this asymptotic behavior turn out to be the solutions of a linear system of three algebraic equations and the resulting tails are efficiently computed. The technique developed makes it possible to analyse with confidence a large class of coplanar transmission lines including several strips or slots embedded in a multilayered bianisotropic medium. Thus, it is possible to study from the simpler microstrip/microslot embedded in a dielectric medium to the much more involved asymmetric strip-like/slot-like coplanar lines embedded in stratified gyroelectric and/or gyromagnetic media. The method is also aware of the numerical drawbacks related to the presence of very thin layers.

Three facts should be emphasized regarding the convergence of the propagation parameters with respect to the basis functions employed in the expansion of the field/current density: a) The typical Chebyshev-type basis functions have shown to be very suitable to study the nonreciprocal lines in case the external magnetization is assumed to be on a plane perpendicular to the propagation direction, b) The aforementioned basis functions provide a slightly worse convergence (but mostly acceptable) when the external magnetization has certain component along the direction of propagation and c) This convergence can become unacceptable for certain critical configurations when the magnetization is that of case b) and the operation frequency is fixed within the frequency forbidden region.

The application of the present method to the analysis of a microstrip with a magnetised-ferrite superstrate has revealed the appearance of certain unidirectional magnetostatic modes. These modes have been found within the range of forbidden frequencies when the external magnetization is on a plane perpendicular to the direction of propagation.

Appendix

Two cases are considered in the computation of expression (22):

- $p = q$

In this case, the integral (22) becomes

$$K^{\pm}_{pnpm,i} = (\pm 1)^{n+m-i}\left(\frac{2}{\omega_p}\right)^{i-1}\int_x^{\infty}\frac{J_n(\alpha)J_m(\alpha)}{\alpha^i}\,d\alpha = (\pm 1)^{n+m-i}\left(\frac{2}{\omega_p}\right)^{i-1}K_{nm,i}(x) \tag{23}$$

with $x = (\omega_p/2)u$. The integral $K_{nm,i}(x)$ is now rewritten as

$$K_{nm,i}(x) = \int_x^{\infty}\frac{J_n(\alpha)J_m(\alpha) - J_n^{\infty}(\alpha)J_m^{\infty}(\alpha)}{\alpha^i}\,d\alpha + \int_x^{\infty}\frac{J_n^{\infty}(\alpha)J_m^{\infty}(\alpha)}{\alpha^i}\,d\alpha = K'_{nm,i}(x) + K''_{nm,i}(x), \tag{24}$$

assuming the following asymptotic behavior, $J_n^{\infty}(\alpha)$, of the Bessel function of order n

$$J_n^{\infty}(\alpha) = \sqrt{\frac{2}{\pi\alpha}}\cos\left(\alpha - \frac{n\pi}{2} - \frac{\pi}{4}\right).$$

The first integral of (24) is numerically computed following the same scheme proposed for the computation of the second and third integral appearing in expression (16). This integral is very fastly convergent assuming the suggested choice of the limit of integration u. Regarding the second integral of (24), it can be expressed in terms of the integral cosine, Ci (x), and integral sine, Si (x), functions as follows

$$K''_{nm,i}(x) = \frac{2^i}{\pi}\left\{\cos\left(\frac{n+m+1}{2}\pi\right)[\text{Ci}\,(2x)]^{i+1} + \sin\left(\frac{n+m+1}{2}\pi\right)[\text{Si}\,(2x)]^{i+1} + \frac{\cos\left(\frac{n-m}{2}\pi\right)}{i(2x)^i}\right\}. \tag{25}$$

- $p \neq q$

Prior to dealing with this case, it should be noticed from (22) that

$$K^{-\infty}_{pnqm,i} = (-1)^{n+m-i}(K^{\infty}_{pnqm,i})^*$$

$$K^{\infty}_{qnpm,i} = (K^{\infty}_{pnqm,i})^*,$$

what implies that only $K^{\infty}_{pnqm,i}$ should be treated. The integration along the real axis k_x in $K^{\infty}_{pnqm,i}$ is transformed into an integration along the imaginary axis jk_x via the

application of the Cauchy theorem, that is

$$K^{\infty}_{pnqm,i} = \int_u^{\infty} \frac{J_n\left(\frac{\omega_p}{2}k_x\right) J_m\left(\frac{\omega_q}{2}k_x\right)}{(k_x)^i} e^{jsk_x}\, dk_x$$

$$= je^{jsu} \int_0^{\infty} \cdot \int_0^{\infty} \frac{J_n\left((u + jk_x)\frac{\omega_p}{2}\right) J_m\left((u + jk_x)\frac{\omega_q}{2}\right)}{(u + jk_x)^i} \cdot e^{-sk_x}\, dk_x \qquad (26)$$

with $s = c_p - c_q$. Note that this last form of the integral is very fastly convergent due to the presence of the negative exponential factor e^{-sk_x}.

REFERENCES

[1] H. Suhl and L. R. Walker, "Topics in guided wave propagation through gyromagnetic media," *Bell Syst. Tech., J.*, vol. 33, pp. 1132–1192, Sept. 1954.

[2] P. S. Epstein, "Theory of wave propagation in a gyromagnetic medium," *Review of Modern Physics*, vol. 28, no. 1, pp. 3–17, Jan. 1956.

[3] B. Lax and K. J. Button, *Microwave Ferrites and Ferrimagnetics*. New York: *McGraw-Hill*, 1962.

[4] G. T. Roome and H. A. Hair "Thin ferrite devices for microwave integrated circuits," *IEEE Trans. Microwave Theory Tech.*, vol. MTT-16, pp. 411–420, July 1968.

[5] M. E. Hines, "Reciprocal and nonreciprocal modes of propagation in ferrite stripline and microstrip devices," *IEEE Trans. Microwave Theory Tech.*, vol. MTT-19, pp. 442–451, May 1971.

[6] J. C. Minor, and D. M. Bolle, "Modes in the shielded microstrip on a ferrite transversely magnetised in the plane of the substrate," *IEEE Trans. Mic. Theory Tech.*, vol. MTT-19, pp. 570–577, July 1971.

[7] R. A. Pucel and D. J. Masse, "Microstrip propagation on magnetic substrates—Part I: design theory," *IEEE Trans. Microwave Theory Tech.*, vol. MTT-20, pp. 304–308, May 1972.

[8] L. Courtois, N. Bernard, B. Chiron, and G. E. Forterre, "A new edge-mode isolator in the very high frequency range," *IEEE Trans. Microwave Theory Tech.*, vol. MTT-24, pp. 129–135, Mar. 1976.

[9] A. Beyer and K. Solbach, "A new fin-line ferrite isolator for integrated millimeter-wave circuits," *IEEE Trans. Microwave Theory Tech.*, vol. MTT-29, pp. 1344–1348, Dec. 1981.

[10] G. Böck, "Dispersion characteristics of slot lines on a ferrite substrate by a mode-matching technique" *Electron. Lett.*, vol. 18, no. 12, pp. 536–537, June 1982.

[11] Y. Hayashi and R. Mitra, "An analytical investigation of finlines with magnetised ferrite substrate," *IEEE Trans. Microwave Theory Tech.*, vol. MTT-31, pp. 495–498, June 1983.

[12] W. Zieniutycz, "Modes of propagation in slot line with layered substrate containing magnetised ferrite," *Electron. Lett.*, vol. 19, no. 4, pp. 966–967, Feb. 1983.

[13] G. Böck, "New multilayered slot-line structures with high nonreciprocity," *Electron. Lett.*, vol. 19, no. 23, pp. 966–967, Dec. 1983.

[14] F. J. K. Lange, "Analysis of shieleded slot lines on lossy multilayered substrates containing a gyromagnetic layer," in *Proc. Int. URSI Symp.*, Santiago de Compostela 1983, pp. 463–466.

[15] S. Tedjini and E. Pic, "Analysis of shieleded slot lines on lossy multilayered susbstrates containing a gyromagnetic layer," in *IEE Proc.*, vol. 131, pt. H, no. 1, pp. 61–63 Feb. 1984.

[16] D. B. Sillars and L. E. Davis, "Coupled-slot fin-line isolators," *Electron. Lett.*, vol. 21, no. 3, pp. 97–98, Dec. 1983.

[17] A. Beyer and I. Wolff, "Design of a millimetre-wave ferrite isolator at 28.5 GHz" in *Inst. Elec. Eng. Proc.*, vol. 132, pt. H, no. 4, pp. 244–249, July 1985.

[18] C. M. Krowne, "Fourier transformed matrix method of finding propagation characteristics of complex anisotropic layered media," *IEEE Trans. Microwave Theory Tech.*, vol. MTT-32, pp. 1617–1625, Dec. 1984.

[19] J. L. Tsalamengas, N. K. Uzunoglu, and N. G. Alexopoulos, "Propagation characteristics of a microstrip line printed on a general anisotropic substrate," *IEEE Trans. Microwave Theory Tech.*, vol. MTT-33, pp. 941–945, Oct. 1985.

[20] B. Janiczak, "Comparative study of the transmission property of planar microstrip structures containing lossy gyromagnetic layer," *Proc. Int. URSI Symp.*, Budapest 1986, pp. 459–462.

[21] E. B. El-Sharawy and R. W. Jackson, "Coplanar waveguide and slot line on magnetic substrates: Analysis and experiment," *IEEE Trans. Microwave Theory Tech.*, vol. 36, pp. 1071–1078, June 1988.

[22] C. M. Krowne, A. A. Mostafa, and K. A. Zaki, "Slot and microstrip guiding structures using magnetoplasmons for nonreciprocal millimeter-wave propagation," *IEEE Trans. Microwave Theory Tech.*, vol. 36, pp. 1850–1859, Dec. 1988.

[23] E. B. El-Sharawy and R. W. Jackson, "Analysis and design of microstrip-slot line for phase shifting applications," *IEEE Trans. Microwave Theory Tech.*, vol. 38, pp. 276–283, Mar. 1990.

[24] E. B. El-Sharawy and R. W. Jackson, "Full-wave analysis of an infinitely long magnetic surface wave transducer," *IEEE Trans. Microwave Theory Tech.*, vol. 38, pp. 730–737, June 1990.

[25] M. Tsutsumi and T. Asahara, "Microstrip lines using yttrium iron garnet film," *IEEE Trans. Microwave Theory Tech.*, vol. MTT-38, pp. 1461–1467, Oct. 1990.

[26] I. Y. Hsia, H. Yang, and N. G. Alexopoulos, "Basic properties of microstrip circuit elements on nonreciprocal substrate-superstrate structure," in *1990 IEEE MTT-S Microwave Symp. Dig.*, pp. 665–668.

[27] T. Kitazawa, "Analysis of shielded striplines and finlines with finite metallization thickness containing magnetised ferrites," *IEEE Trans. Microwave Theory Tech.*, vol. 39, pp. 70–74, Jan. 1991.

[28] F. Mesa, R. Marques, and M. Horno, "A general algorithm for computing the bidimensional spectral dyadic Green's function: The equivalent boundary method (EBM)," *IEEE Trans. Microwave Theory Tech.*, vol. 39, Sept. 1991.

[29] F. Medina, M. Horno, and H. Baudrand, "Generalized spectral analysis of planar lines on layered media including uniaxial and biaxial dielectric substrates," *IEEE Trans. Microwave Theory Tech.*, vol. 37, pp. 504–511, Mar. 1989.

[30] G. Cano, F. Medina, and M. Horno, "Efficient spectral domain analysis of generalized multistrip lines in stratified media including thin, anisotropic and lossy substrates," *IEEE Trans. Microwave Theory Tech.*, vol. 40, pp. 217–227, Feb. 1992.

[31] N. K. Das and D. M. Pozar, "Full-wave spectral-domain computation of material, radiation, and guided wave losses in infinite multilayered printed transmission lines," *IEEE Trans. Microwave Theory Tech.*, vol. 39, pp. 54–63, Jan. 1991.

[32] F. L. Mesa, "Study of the electromagnetic propagation characteristics in multiconductor lines of planar configuration embedded in bianisotropic layered media," Ph.D. dissertation, (in Spanish), Universidad de Sevilla, 1991.

[33] L. M. Delves and J. N. Lyness, "A numerical method for locating the zeros of an anlytic function," *Math. Comput.*, vol. 21, pp. 543–560, 1967.

[34] M. S. Sodha and N. C. Srivastava, *Microwave Propagation in Ferrimagnetics*. New York: Plenum, 1981.

[35] F. Mesa, R. Marques and M. Horno, "Rigorous analysis of nonreciprocal slow-wave planar transmission lines," in *Proc. 21 European Microwave Conf.*, Stuttgart, Germany, Sept. 1991.

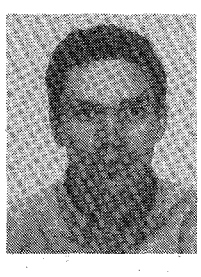

Francisco L. Mesa was born in Cádiz, Spain, on April 1965. He received the Licenciado degree in June 1989 and the Doctor degree in December 1991, both in Physics, from the University of Seville, Spain.

He is currently Lecturer of Physics and member of the Microwave Group in the Department of Electronics and Electromagnetism, University of Seville. His research interests focus on electromagnetic propagation in planar lines with general anisotropic materials.

Ricardo Marqués was born in San Fernando, Cádiz, Spain. He received the degree of Licenciado in Physics in June 1983, and the degree of Doctor in Physics in July 1987, both from the University of Sevilla.

Since January 1984, he has been with the Department of Electronics and Electromagnetism at the University of Sevilla, where he is currently Associate Professor in Electricity and Magnetism. His main fields of interest include MIC devices design, wave propagation in anisotropic media and electromagnetic theory.

Manuel Horno (M'75) was born in Torre del Campo, Jaén, Spain. He received the degree of Licenciado in Physics in June 1969, and the degree of Doctor in Physics in January 1972, both from the University of Seville, Spain.

Since October 1969 he has been with the Department of Electricity and Electronics at the University of Seville, where he became an Assistant Professor in 1970, Associate Professor in 1975 and Professor in 1986. He is a member of Electromagnetism Academy of M.I.T. (Cambridge). His main fields of interest include boundary value problems in electromagnetic theory, wave propagation through anisotropic media, and microwave integrated circuits. He is presently engaged in the analysis of planar transmission lines embedded in anisotropic materials, multiconductor transmission lines, and planar slow-wave structures.